JSR
Journal of Sedimentary Research, 2025, v. 95, 405–416
Research Article
DOI: 10.2110/jsr.2024.021

FIELD TESTING AUTOGENIC STORAGE THRESHOLDS FOR ENVIRONMENTAL SIGNALS IN THE STRATA OF THE MISSISSIPPI RIVER DELTA, U.S.A.

UDITA MUKHERJEE AND KYLE M. STRAUB
Department of Earth and Environmental Sciences, Tulane University, New Orleans, Louisiana 70118, U.S.A.
e-mail: umukherjee@tulane.edu

ABSTRACT: **Sediments transported from source terrains to depositional sinks carry environmental signals, which may or may not be preserved in stratigraphy. Existing theory suggests that storage thresholds for environmental signals are set by the internal dynamics of sediment transport systems. We test this theory by exploring whether changes in relative sea level (RSL) of various scales produce detectable signals stored in field-scale strata. This field test builds on results from physical experiments where identifiable stratigraphic signals of RSL change were produced only from RSL cycles with magnitudes and/or periodicities greater than the spatial and temporal scales of the internal dynamics of deltas. Published long-term sedimentation rates and sea-level reconstructions suggest that the Mississippi River Delta (MRD) should be a good place to study sea-level-signal storage thresholds. We use publicly available seismic volumes from NAMSS-USGS, comparing strata of the late Miocene (LM) and early Quaternary (EQ), to study effects of paleo–sea-level change on the dimensions of channelized bodies in the MRD. Calculating dimensionless depth and time scales, we show that the likelihood that EQ channelized bodies store signals of relative sea-level change is higher than that in the LM channelized bodies. Observations lead to interpretations of paleovalleys preserved in the EQ strata, but not in the LM strata, which broadly supports predictions from signal-shredding theory. This study adds field-scale observations that quantify the intermingling of stratigraphic products of internal dynamics with products of RSL change over geologic timescales and underscores the need to appreciate stochasticity in surface processes when building hypotheses related to the stratigraphic record.**

INTRODUCTION

Stratigraphic architecture records past environmental changes (as in, signals) at a variety of scales. We define signals of environmental change as attributes of a landscape's structure, sediment transport capacity, and/or stratigraphic characteristics that can be linked directly to large-scale environmental forcings (e.g., production of accommodation), following Straub et al. (2020). However, these signals potentially can be distorted due to temporary deposition in transient landscape features, in essence spreading the signal across time and space in a source-to-sink system. Significant temporal and spatial spreading of signals can make it impossible to piece together the depositional clues one uses to infer paleo-environmental change. Signal-shredding is the concept that signals of environmental change can be degraded during transport or burial or lose detectability due to the intermingling of the products of allogenic and autogenic surface processes in strata. This theory and experimental tests of the theory are still in their infancy (Jerolmack and Paola 2010; Romans et al. 2016; Griffin et al. 2023) and field application of these ideas is extremely rare.

Relative sea-level (RSL) change is one of the most important external (allogenic) forcings affecting sediment deposition rates and stratigraphic architecture of continental margin systems (Vail et al. 1977; Van Wagoner et al. 1990; Blum and Törnqvist 2000; Karamitopoulos et al. 2014). It is also used as a proxy to reconstruct past change in global temperature, melting of ice sheets, tectonics, and paleogeography (Haq et al. 1987; Fairbanks 1989; Haq 1991; Clark et al. 2004; Alley et al. 2005). However, recent work questions the ability of some basins to record detectable signals of certain RSL events. For example, Li et al. (2016) and Yu et al. (2017), using physical experiments, explored the distortion and reduction in detectability of RSL signals by processes that are intrinsic to sediment transport systems (autogenic processes). This contrasts with many interpretations of sequence-stratigraphic patterns that emphasize deterministic system responses to past RSL change and the resultant stratal architecture (Posamentier and Vail 1988; Posamentier and Allen 1992; Catuneanu et al. 2009). The distinction between allogenic and autogenic controls on sediment transport and the comparison of scales of the resulting stratigraphic features are important questions worth exploring (Best and Ashworth 1997; Ganti et al. 2019). Some observational work (Trower et al. 2018) has even applied aspects of stochastic signal-degradation theory (signal-shredding theory) at field scale.

Channels respond to relative sea-level change, and when these changes are large enough, significant incision and subsequent infilling leaves behind paleovalleys which can be identified in the architecture of strata. The signal of changing relative sea level should thus be preserved in the dimensions of these channels and paleovalleys (Fig. 1), and these signals are thought to be abundant in marginal marine strata (Blum and Törnqvist 2000; Miller et al. 2005; Khan et al. 2019). A change in relative sea level is an environmental forcing that can generate a signal that does not need to

Published Online: April 2025
 1527-1404/25/095-405

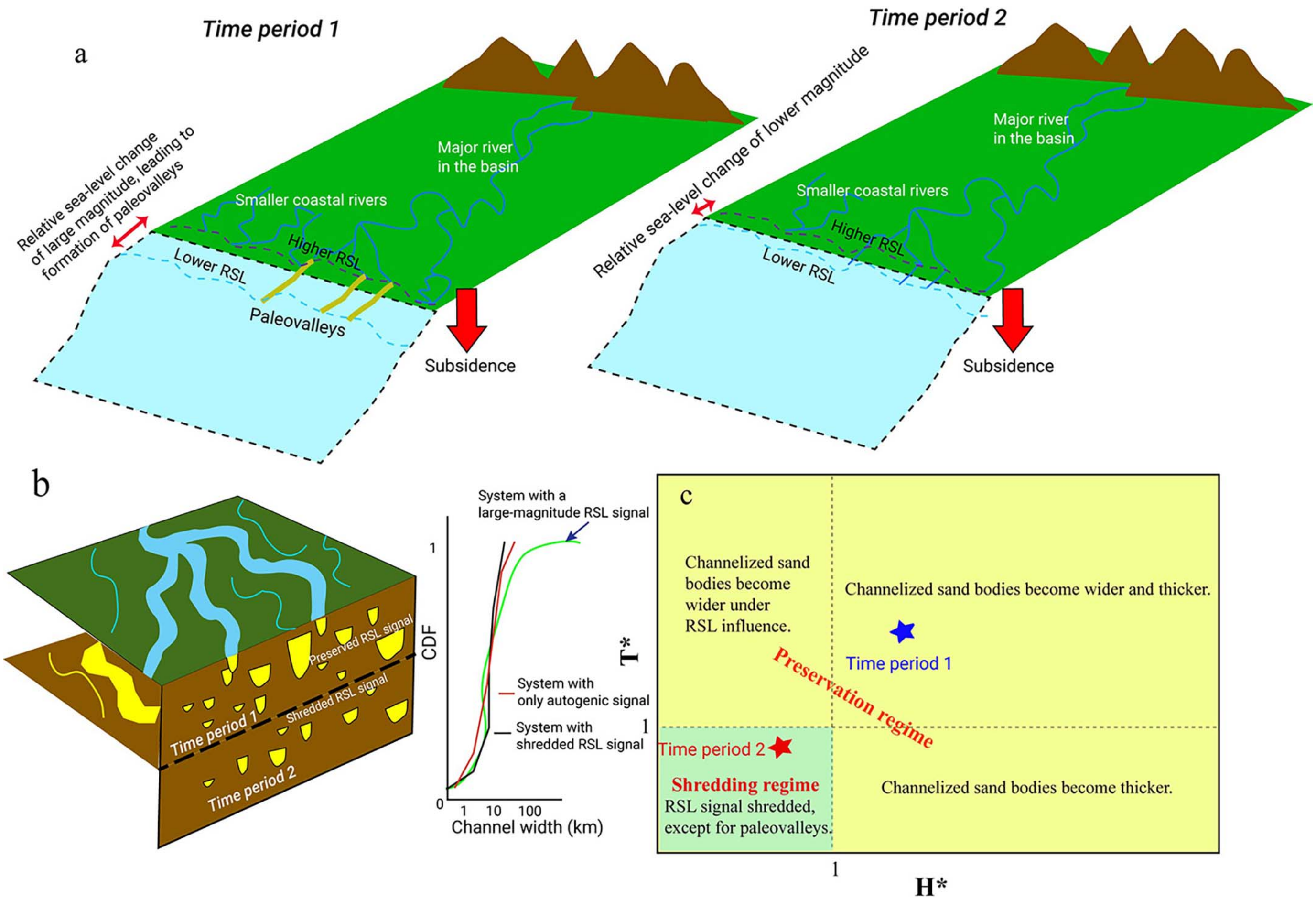

FIG. 1.—Conceptual diagram of a coastal system responding to different relative sea-level changes at different time periods and the resulting distribution of their channelized-body dimensions. **A)** A source-to-sink system responding to a larger RSL change (time period 1), when there is a higher chance of formation of paleovalleys vs. the same system responding to a smaller RSL change (time period 2) without paleovalley formation. **B)** The comparison of both these time periods in a preserved stratigraphic section. The stratigraphy for time period 1 has a larger number of channelized bodies preserved. These are also wider and deeper compared with those from time period 2, where the general distribution is fewer in number as well. **C)** A representation of expected cumulative density distribution of channel widths between a system with only autogenic signals, one with a shredded RSL signal, and another with a large-magnitude RSL signal, akin to the RSL signal in time period 1 (shown in green, with an elongated tail representing much wider CBs). **D)** A representative H*–T* regime diagram, with the position of a large CB plotted for the time periods 1 (plotted in the preservation regime) and 2 (plotted in the shredding regime). The light green area represents the shredding regime, and the yellow area represents the preservation regime.

travel horizontally across the Earth's surface before preservation in strata. Thus, these signals might be spread across only time (and not space) as it is felt by the transport systems first at the shoreline, where subsidence and sea-level rise can generate the accommodation necessary for long term storage (Fisk and McFarlan 1955; Lamb et al. 2012; Voller et al. 2012). During burial, signals first reside in the active layer (layer still susceptible to reworking via autogenic processes) where they can be degraded by the burial and/or incision process. If this degradation is significant, the resultant strata may not preserve detectable evidence of changing RSL, in this case due to incision into existing channelized bodies. Only when these deposits are buried to a depth sufficient to be shielded from autogenic surface processes are they safe from further autogenic degradation (Mohrig et al. 2000; Olariu and Bhattacharya 2006; Straub et al. 2009). In addition to degradation due to autogenic reworking, variability in stratigraphic products due to allogenic forcing might not be detectable in strata if the scales of the environmental signals are similar to the scales of autogenic products, which Griffin et al. (2023) termed signal obscuring. The work detailed here focuses on degradation and obscuring of RSL signals resulting from reworking during burial and intermingling of allogenic signals with autogenic processes, specifically for signals with short horizontal transit distances (RSL signals preserved near paleo-shorelines).

We use a publicly available seismic volume, BA-57-93-LA from the National Archive of Marine Seismic Surveys, under USGS (NAMSS-USGS) (Fig. 2) to measure the dimensions of stratigraphic features resulting from channelized flow in the strata of the EQ and the LM. We ascertain if any of these channelized geobodies (CBs) can be categorized as paleovalleys in the sedimentary packages from the two time periods of interest, which is indicative of the storage of sea-level signals. Predicting signal detectability requires estimates of autogenic system scales. To accomplish this, we first define autogenic scales, from the dimensions of the present-day Mississippi River which is largely the result of autogenic processes that have played out over the Holocene (Blum and Törnqvist 2000; Li et al. 2016; Yu et al. 2017). We then look for variations away from these autogenic scales in the Mississippi River strata. To our knowledge this is the first field-scale study to test signal-shredding theory.

The past physical and numerical experiments used to test signal-shredding theory assumed that the major trunk system in a sedimentary

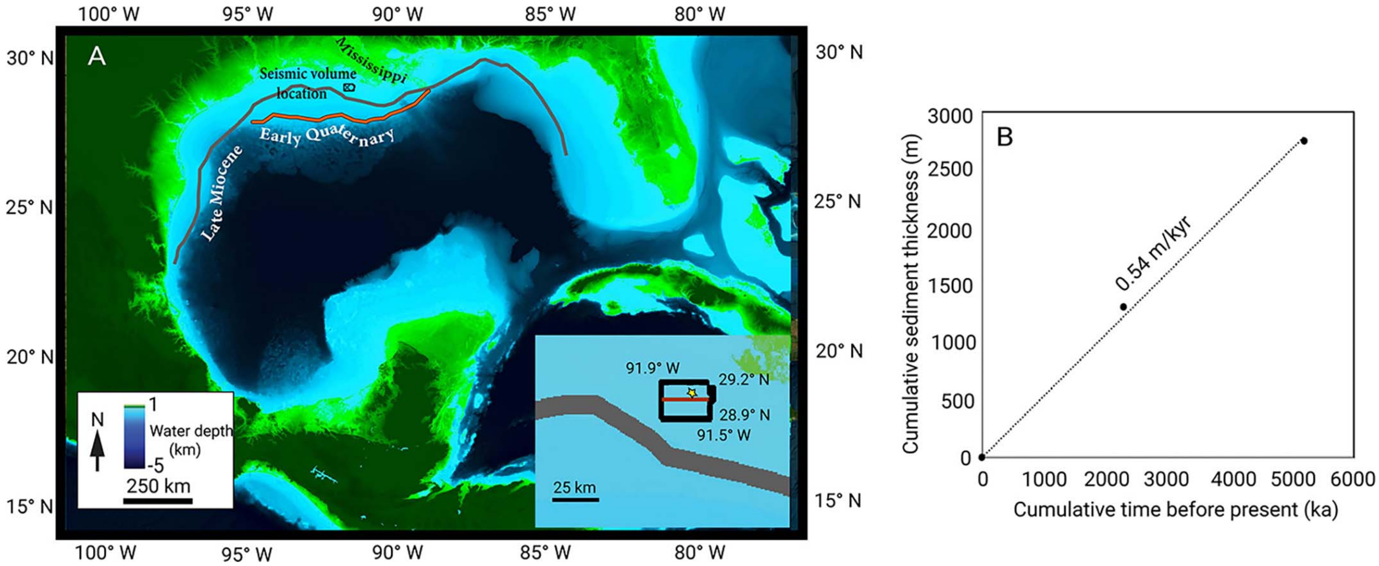

FIG. 2.—**A)** Map of the study area. The red line is the extent of the continental shelf edge during the early Quaternary, and the dark gray line is the location of the shelf edge during the late Miocene. The study area was inboard of the shelf edge during both times. The inset shows the boundary for the seismic survey (B-57-93-LA) used in the study, the location of the transect of the dip section shown in Figure 3 (red line), and the location of the well referred in Part B (yellow star). **B)** Age vs. sediment thickness for Well API # 177094078100 in the study region. Age data were determined for biostratigraphic markers and best-fit trend line gives a long-term sedimentation or subsidence rate of 0.54 m/kyr. The planktonic microfossils were recovered from well API#177094078100, with data made publicly available by U.S. Department of the Interior, Bureau of Ocean Energy Management.

basin sets the fidelity of the entire basin. These experiments were fed by a single delivery point for water and sediment to the experimental basins (Li et al. 2016; Yu et al. 2017). However, we recognize that the larger MRD basin contains both a trunk channel system and smaller coastal river basins (Swartz et al. 2022; Cardenas et al. 2023). Thus, we also explore the ability to detect signals in deposits of these small coastal systems that exist in the larger basin. We hypothesize that EQ RSL signals will be preserved in strata deposited from both the small and large systems. In contrast, signals of LM RSL change are expected to be preserved in strata deposited from the smaller coastal systems, but not in the strata tied to the trunk system.

THEORETICAL BACKGROUND

To test our hypothesis, we need to compare the allogenic length and time scales (e.g., amplitude and time periods of RSL cycles) with the autogenic time and space scales affecting the CBs. Following theory developed by Li et al. (2016) and Yu et al. (2017), we developed a framework for testing RSL signal preservation in strata, using two dimensionless numbers: H^*, a dimensionless length scale, and T^*, a dimensionless timescale (Li et al. 2016; Yu et al. 2017). This framework has been utilized to quantitatively compare the scales of allogenic environmental forcings with the scales of local autogenic products, reflected in the dimensions of channelized bodies. They are defined as:

$$H^* = \frac{R_{RSL}}{H_C} \tag{1}$$

$$T^* = \frac{T_{RSL}}{T_C} \tag{2}$$

where R_{RSL} is the range of an RSL cycle (i.e., difference in elevation of sea level between highstand and lowstand), H_C is the depth of the largest autogenic channels, which can be as large as $3H_{mean}$ (Ganti et al. 2014), T_{RSL} is the period of an RSL cycle, and T_C is the compensation timescale, which is the time for deposits of autogenic surface processes to average out such that an isopach reflects an accommodation-generation pattern (Wang et al. 2011). The compensational timescale can be estimated as

$$T_C = \frac{l}{\bar{r}} \tag{3}$$

where $\bar{r}$ is the long-term sedimentation rate and l is the maximum autogenic vertical roughness scale in a region of study. In several experimental studies, l has been approximated by H_C and thus defined by the depth of the largest autogenic channels. However, this scale for some settings might be larger than H_c, due to the presence of features like delta foresets that could introduce larger roughness scales into a system (Trampush et al. 2017). We use maps of the lower Mississippi River (Nittrouer 2013; Fernandes et al. 2016) to estimate an H_c of $\sim$ 70 m. Previous estimates of a long-term sedimentation (or subsidence) rate of 0.23 m/kyr for this system came from biostratigraphic dates in the strata below the current Bird's foot of the MRD (Straub et al. 2009). Using these values, estimates of H^* and T^* for the MRD EQ are 1 and 0.1, respectively, whereas for LM strata, H^* and T^* are estimated at 0.2 and 0.1, respectively.

The H^*–T^* regime can aid prediction of not only the presence, but also an expected type of RSL signal in strata, depending on the RSL signals falling in the different quadrants of the H^*–T^* space (Fig. 1). H^* and T^* are inversely proportional to autogenic channel depths (Eqs. 1 and 2). A channel that plots in the quadrant defined by both H^* and $T^* > 1$ should produce CBs that are both deeper and wider than their autogenic representations. In the case of $H^* > 1$ and $T^* < 1$, we suggest the dominant signal will be an increase in CB thickness relative to autogenic products as the high RSL cycle amplitude will be linked to incision, but there will be limited time to widen the valley during the falling or low RSL portion of a cycle. For $T^* > 1$ and $H^* < 1$, one can expect to see wider CBs but not necessarily channel bodies that are thicker than autogenic scales. In the case of H^* and T^* both being less than 1, the RSL signal will be susceptible to shredding or of similar scale to products of autogenic processes, making them difficult to detect.

STUDY AREA

When it comes to exploration of signal-shredding theory at field scales, little has been done because of the scarcity and/or lack of exploration of publicly available 3-D data that has decent areal coverage and is sufficiently dated. Li et al. (2016) and Yu et al. (2017) calculated the preservation potential of RSL signals for a database of field-scale deltaic systems. This analysis suggests that the present-day Mississippi River Delta (MRD) is a good place to test signal-shredding theory. RSL cycles from two time periods in the large basin of the MRD are hypothesized to reside on either side of the divide between the stratigraphic signal detection. Specifically, we compare strata deposited during the early Quaternary (EQ), when RSL cycled with large amplitudes, and the late Miocene (LM), which had much lower-amplitude RSL cycles (Lisiecki and Raymo 2005; Miller et al. 2005).

While the sediment routing and drainage patterns of the Mississippi River changed through time, the MRD has been active for most of the last 65 Myr (Galloway et al. 2011; Blum and Pecha 2014; Blum et al. 2017; Xu et al. 2017). During the LM and EQ time periods, the terminus of the Mississippi River was one of the principal depocenters in the Gulf of Mexico (Galloway et al. 2011; Bentley et al. 2016; Blum et al. 2017; Xu et al. 2017).

The present axis of the MRD has been in place since the Miocene. During this time, RSL cycles ranged from ~ 10–20 m with a cycle period of ~ 40 kyr (Lisiecki and Raymo 2005; Miller et al. 2005; Raymo et al. 2006). The shelf edge prograded by ~ 200 km, and the nucleus for the present alluvial system, with the deepwater system in the Gulf of Mexico, was set up (Winker 1982; Galloway et al. 2011).

Throughout much of the early Quaternary (2.5–0.77 Ma), RSL cycles were still dominated by a 40 kyr period. This transitioned to a dominant period of 100 kyr in the Pleistocene (Imbrie and Imbrie 1980; Lisiecki and Raymo 2005; Miller et al. 2005; Raymo et al. 2006). EQ RSL cycles had a range of ~ 60–70 m (Lisiecki and Raymo 2005; Miller et al. 2005; Raymo et al. 2006). During this period, the mean Quaternary shoreline rested around the present-day mid-shelf with superimposed fluctuations due to the RSL forcing (Blum and Hattier-Womack 2009).

The MRD basin has been impacted by shifts in climate and associated sea-level change over a range of timescales (Buzas-Stephens et al. 2014). Possibly the largest environmental forcing at this site is eustatic sea level (Fisk and McFarlan 1955; Blum and Törnqvist 2000), given its influence on the location of shorelines and the change of transport physics that occur across this boundary.

Over long timescales, depositional patterns in the MRD are influenced by changes in sediment flux from the hinterland (Anderson et al. 2016), differential fluvial fluxes (Olariu and Steel 2009), variable basin subsidence in space and time, driven by sediment compaction, and glacial and sedimentary isostatic adjustment (Törnqvist et al. 2008; Anderson et al. 2016), oceanographic currents and circulation systems (Anderson et al. 2004, 2016), and structural processes due to deep-seated subsidence caused by cooling of the crystalline basement and movement of gravity tectonic structures (e.g., Jurassic Louann salt) (Galloway 2008; Peel 2014). The salt and the structures created by its movement add to the overall complexity of the MRD (Winker 1982; Diegel et al. 1995; Peel et al. 1995; Galloway et al. 2000; Combellas-Bigott and Galloway 2006; Peel 2014) and care has been taken to exclude manifestations of the salt structures and faults during seismic interpretation (Fig. 3).

DATA AND METHODS

Age Control

To meaningfully analyze the geologic history contained in the seismic stratigraphy in the study area, age control of the strata is needed. There is limited age control in the study area over the age range we query. However, for this study, the precise age of strata that might allow one to identify the signal of a specific sea-level cycle is not necessary. Rather, sufficient dating that allows for the general age of strata (± 1 Myr) is necessary. This allows us to identify the general scale (amplitude and period) of sea-level fluctuations that were ongoing at the time of deposition. By using planktonic foraminifera available from a well (API # 177094078100) in the study area, an age–depth model is generated (Fig. 2B). Specifically, using the depth and age ranges of the microfossils *Lenticulina* and *Bigenerina floridana* in conjunction with the modern Earth surface, the estimated sedimentation rate for the study area is 0.54 m/kyr. Using this rate, the estimated local H^* and T^* values for the EQ are 1 and 0.8, respectively, whereas for LM stratigraphy H^* and T^* are 0.1 and 0.8, respectively.

Present-Day Mississippi Channel Width

The dimensions from the present-day Mississippi channel were compared to the EQ and LM CB dimensions. Data defining the depth and width of the present-day Mississippi channel, as measured from Head of Passes, are reported in Nittrouer et al. (2013) (collected by U.S. Army Corps of engineers (USACE; data collected 1974–1975; found in Harmar 2004, appendix)). This survey data includes channel cross sections on average every 312 m, which covers the transition from the normal-flow stretch through the backwater reach. The difference in channel–levee crest and thalweg elevations for every transect are reported as modern channel depths. The width data come from these same profiles and are measured from one levee crest to the levee crest on the opposite channel margin along a perpendicular transect. All the elevation data are expressed in meters above mean sea level and were converted from the data referenced to NGD 1929. Distributions of channel depths and widths are then generated for the lower 800 river kilometers and for just the lower 200 river kilometers.

The distance of the farthest landward edge of the seismic volume from the average LM and average EQ shoreline are ~ 120 km and ~ 50 km, respectively. These are calculated based on the perpendicular distance of the center of the seismic volume from the closest EQ and LM shoreline positions (Galloway et al. 2000). Acknowledging that sea-level cycles, sediment supply, and accommodation can alter these distances significantly, this is an estimate of the average distance separating the study region from the shoreline over the time periods explored, and comparable to the lower 200 river kilometers of the present-day Mississippi channel belt.

Channel belt width data from Fernandes et al. (2016) is then used to compare EQ and LM CB dimensions with modern autogenic values. Again, distributions of CB scales are made both for the lower 800 km and lower 200 km. Given the time integrative nature of strata, the scales of interpreted CBs are likely more analogous in their formative processes to modern channel belts, compared to the geometry of the river itself.

Channel-Body Mapping

The publicly available 3-D seismic cube, BA-57-93-LA (~ 980 km^2), used here to generate distributions that describe widths and depths of CBs, covers a swath of the current continental shelf, just west of the Mississippi Canyon (Figs. 2, 3). This region is near the center of the long-term MRD basin (Fig. 2A) and as such received sediments through the LM and EQ time periods (Galloway 2008; Galloway et al. 2000, 2011). The seismic volume was collected in 1993 for purposes of oil and gas exploration. The inline and crossline spacings are 25 m, and the sample interval is 4 milliseconds. The frequency content of the seismic volume averages ~ 35 Hz with a fall-off on the high frequency end at ~ 65 Hz, with a theoretical

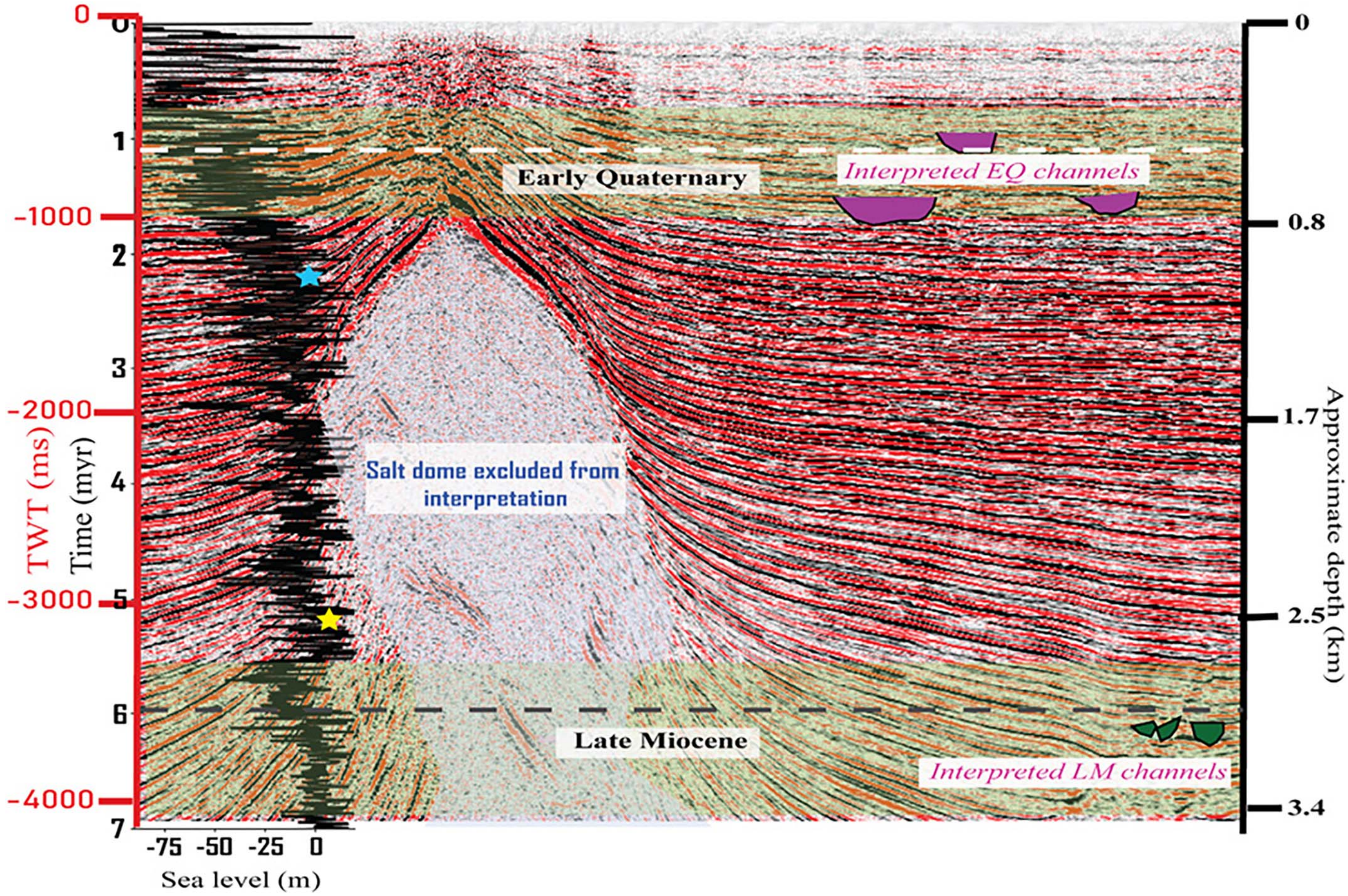

FIG. 3.—A dip section showing the relationship of two-way travel time and depth with respect to the relative sea-level history adapted from Miller et al. (2005). The blue star shows the presence of an early Quaternary, EQ, microfossil which is used to constrain the time period of interest in the EQ. The specific window of EQ strata analyzed is demarcated by the colored box labeled early Quaternary. The late Miocene, LM, stratigraphy has been constrained from foraminifera samples, shown by a yellow star, which constrains the age of the time period of interest right below, shown by the colored box labeled late Miocene. Examples of CBs interpreted in the vertical sections for both EQ and LM are shown. The white dashed line shows the approximate location of the time slice shown in Figure 2A as an example of EQ stratigraphy and the black dashed line is the same shown in Figure 5 for the late Miocene.

vertical resolution of 7–14 m. Using the calculated sedimentation rate, EQ strata (1–0.8 Ma) are in a depth range of 0.5–1 km. For LM strata (6–6.3 Ma), the depth range is 3.5–4 km. However, the uncertainties on these numbers can be expected to be large, because the sedimentation rate is likely somewhat variable even in the million-year temporal resolution. The sedimentation rate calculated here is an average for the basin, which is based on three micropaleontological dates. But this does not rule out the possibility of sudden increased pulses of sedimentation, caused by transience of tectonic or climatic states in the basin, which could have affected both sediment flux to the depositional basin and the accommodation available.

Seismic waves are reflected and refracted along geophysical boundaries, many of which are associated with lithologic boundaries in the subsurface. Using this principle, the seismic cube was utilized to interpret CBs of dimensions different from the EQ and LM. For this study, we define channelized bodies as any geobody constructed from channelized processes and encompasses channels, channel belts, and paleo-valleys. We emphasize and acknowledge that this is slightly different than how the term is commonly used in the literature. However, we do not assume the genesis of these channelized bodies; we base our analysis only on the distributions of the stratigraphic bodies with channelized features. These CBs were interpreted from both horizontal and vertical seismic sections. Interpretation and mapping of the smaller channel features is easier in approximately horizontal time slices compared to vertical sections due to data resolution and the typical aspect ratio of CBs (width $\gg$ depth). CB margins are interpreted on horizontal (time) sections using a variance attribute that accentuates edges or discontinuities in the seismic data (Figs. 4, 5). Windows of $\sim$ 100 milliseconds, which corresponds to about 300,000 years of age and close to 100 m of thickness, are identified for both the EQ and LM time periods. This thickness is roughly equivalent to the compensation scale of the basin (i.e., approximately equal to the maximum depth of the modern Mississippi River). Each of these windows is then divided into 12 time slices with a spacing of 8 milliseconds, with the LM sections flattened on a regional surface. For every time slice, discontinuities interpreted as CB margins were mapped. CB margins are described as two linear features that run approximately parallel to each other with a relationship of sinuosity to channel width similar to modern-day channels and channel belts (Leopold and Wolman 1960). Some CBs were also mapped in cross section where they were identified with paired inclined reflectors that truncate underlying seismic horizons. This mapping process produced a database that consists of 821 CBs: 431 (50 vertically resolvable from seismic data) from EQ and 390 (33 vertically resolvable from seismic data) from LM. Using the interpreted CB margins, channelized-body widths were calculated using a Python-based script designed by Sylvester and reported on in Sylvester et al. (2021). The

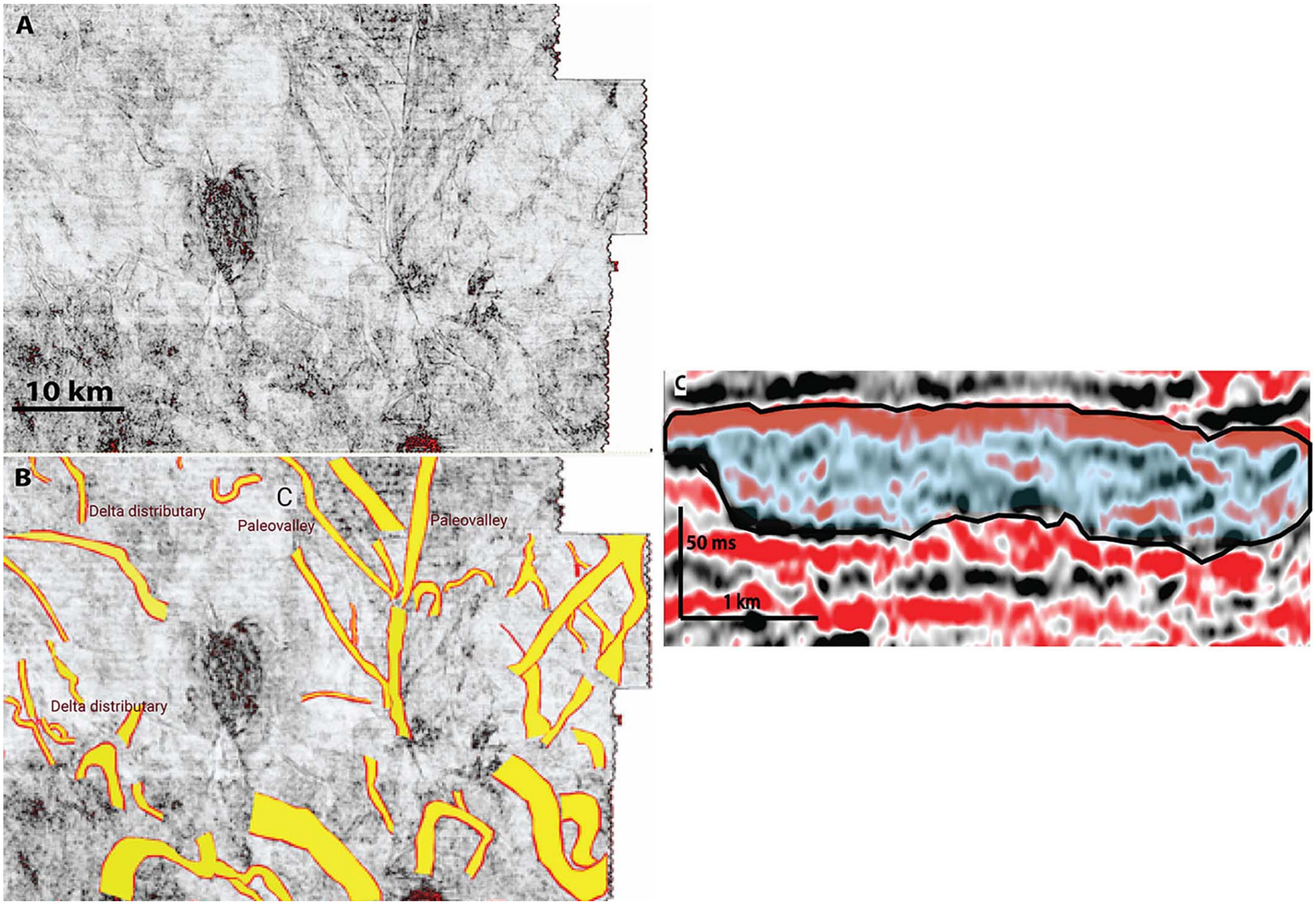

FIG. 4.—A variance time slice (600 ms) from EQ time period. **A)** The uninterpreted section and **B)** the interpreted CBs in yellow. **C)** An example of an interpreted paleovalley.

script and explanation for the width calculation is available at https://github.com/zsylvester/channelmapper.

Following the Gibling (2006) framework, geobodies produced by channelized transport processes in coastal settings can be placed into four bins: alluvial valley fills, delta distributaries, meandering channels, and braided channels. The calculated CB widths were compared with the typical widths of these types of features, as reported by Gibling (2006) (Table 1) and then interpreted accordingly.

We estimate thicknesses of CBs, specifically maximum thicknesses, which are necessary to calculate H^* and T^*. CBs with thicknesses below the vertical resolution of the seismic volume cannot be directly interpreted. For each CB that could not be imaged in the vertical, we used the database from Gibling (2006) to calculate a theoretical maximum CB thickness. Depending on the type of CB, the width was combined with the associated width:thickness ratios to arrive at a theoretical maximum thickness (Table 1). For vertically resolvable CBs, the difference between the maps of the CB base and an approximate top envelope gives an approximate maximum thickness. The top envelope is constructed by connecting the top elevation of paired CB margins.

H^* and T^* for all CBs are calculated using equations 1 and 2. This is an important distinction with the works done by Li et al. (2016) and Yu et al. (2017), who calculated H^* and T^* for a depositional basin using the depth of the deepest channel observed on the experimental surface.

RESULTS

Channelized-Body Dimensions

Classification based on the definitions of Gibling (2006) suggests that CBs interpreted in both EQ and LM are either delta distributaries or meandering channels, with only a small section of these being braided channels (Fig. 6). Even though this method creates very sharp boundaries between the different types of CBs, we want to emphasize that in nature these boundaries are gradational. Difference in the types of CBs between the two time periods are apparent only in the upper tails of the distributions. The cumulative distributive functions (CDF) of the widths of CBs from the EQ and LM are similar, spreading over scales of 10^1–10^3 m. However, the EQ distribution contains several CBs that approach widths of 10^4 m (Fig. 6). These exceptionally wide EQ CBs are interpreted as paleovalley fills. The LM strata lack these exceptionally wide CBs. These wide EQ CBs are also exceptionally thick (Fig. 6). The thickness of the CBs from both EQ and LM are between 10^1 and 10^2 m, except for the wide EQ CBs whose estimated maximum thicknesses are between 10^2 and 10^3 m. Given uncertainty in the width-to-depth conversion used, a number of these CBs might be thinner than reported here.

Next, width-to-thickness ratios were calculated for the CBs resolvable in vertical seismic sections (Fig. 7). Almost all CBs from the EQ have a width-to-depth ratio between 1 and 60, with two being more than 100. In comparison, all but one of the LM CBs have width-to-thickness ratios between 1 and 40, with the outlier being 80. The thickest EQ and LM CBs

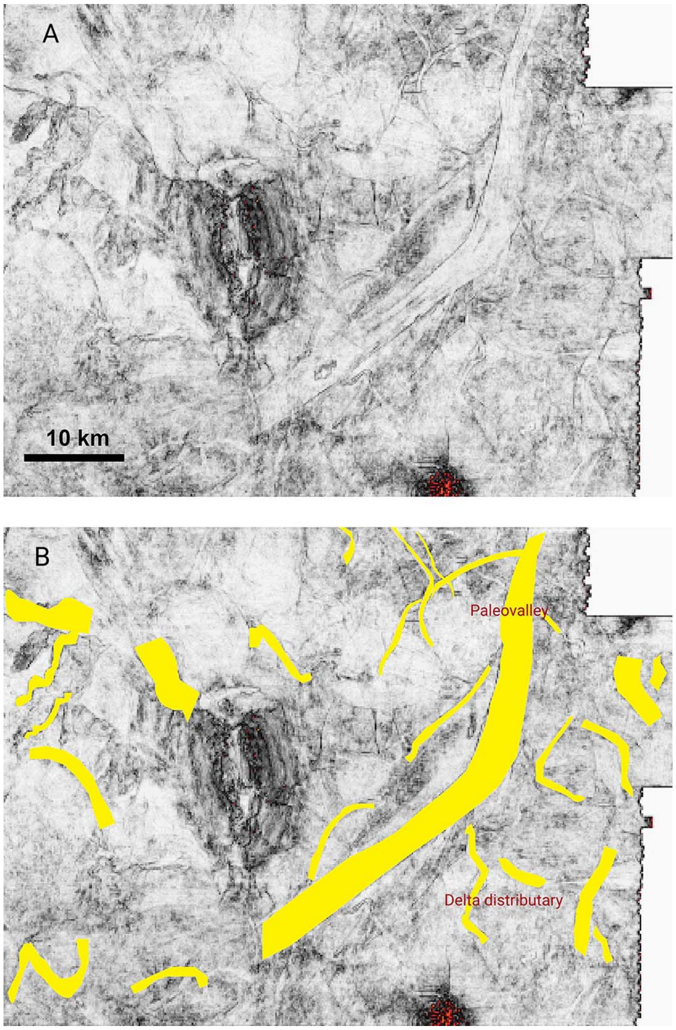

FIG. 5.—A variance time slice from the LM time period. **A)** The uninterpreted section and **B)** the interpreted CBs in yellow.

($>$ 100s of m) show low width-to-thickness values ($<$ 5) (Fig. 7). The width-to-depth ratio of the present-day Mississippi River varies between 1 and $\sim$ 400, but for the part downstream of the backwater length i.e., $\sim$ 0–300 river kilometers, this ratio is $<$ 40 (Blum et al. 2013), which compares well with the width-to-thickness ratios of the LM CBs reported here. The widths of paleovalleys are commonly more than 100 times their thickness (Gibling 2006). That signature can be seen in only two CBs in this dataset, and both are from the EQ.

Utilizing the measurements of maximum channel depths and local subsidence rates, H^* and T^* were estimated. We present these measurements in an H^*–T^* space that is divided into four quadrants, based on the values of both the time and depth scales of RSL signal preservation. Plotting in the signal-shredding regime, $<$ 5% of the EQ CBs have both H^* and $T^* < 1$, and the rest of the CBs have either $H^* > 1$ or both H^* and T^* greater than 1. This suggests that CBs from these time periods have a significant chance of containing signals of changing RSL. The EQ CBs with the lowest H^* and T^* values are interpreted as paleovalleys from their geometries, and thus their scales are likely the result of sea-level-driven allogenic processes. In comparison, $\sim$ 40% of the LM CBs plot in the shredding regime, with only one LM CB having $H^* > 1$ and 60% of them $T^* > 1$. Close to half of the total population of interpreted LM CBs are expected to shred the RSL signal. Further, all of

TABLE 1.—*The dimensions and their ratio used in the analysis to interpret types of channelized bodies and calculate their thickness, following Gibling (2006).*

Types of Channels	Common Range for Width (km)	Maximum Width to Depth Ratio
Delta distributaries	0.01–0.3	1:5
Meandering	0.3–3	1:30
Braided/low-sinousity rivers	0.5–10	1:50
Valley-fills within alluvial and marine strata	0.2–25	1:10

the larger CBs fall in the shredding regime and do not have width and depth statistics indicative of paleovalleys.

To estimate uncertainties in H^* and T^* values, a lower sedimentation rate of 0.26 m/kyr (reported by Straub et al. (2009) from the southeastern part of the Mississippi River Basin) was used to calculate the same suite of statistics as discussed above (Fig. 8). With the lower sedimentation rate, all but one LM CBs plot in the shredding regime. For the EQ $<$ 5% of the CBs plot in the shredding regime, with the rest having $H^* > 1$. Almost 95% of the EQ CBs are expected to store the RSL signal in this case.

Present-Day Mississippi Channel Width

The dimensions of the present-day Mississippi River channel and channel belt are compared with CBs from both the LM and EQ. Only a few of these EQ and LM CBs, which are a collection of channelized sediment transport systems of varying scales, are comparable to the present-day Mississippi-scale system. The important observation is that the thicker and wider CBs present in the EQ make the upper tails of the distributions heavier compared to that of the modern channel, channel belt, or the upper tail from LM (Fig. 9). The dimensions of the present-day autogenic Mississippi River channel and channel belt downstream from the backwater reach are smaller than the dimensions of the interpreted paleovalleys seen in the upper tail of the EQ CBs. The width and the thickness of the EQ paleovalley features are close to a factor of two larger than anything seen in the LM distribution and the present-day Mississippi River. Thus, the dimensions of the present-day autogenic Mississippi River channel are closer to those found in the distribution of CB dimensions from the LM (Fig. 9A). This supports an interpretation that the LM strata dominantly stores autogenic process signals, while allogenic RSL signals are likely lacking due to shredding by autogenic processes. Even though the modern-day Mississippi channel belt width is smaller than that of the heavier tail of the EQ CBs, the scales of these features are closer in size than that of the present-day Mississippi River (Fig. 9B).

DISCUSSION

The measured (and estimated) width and thickness of CBs from the EQ and LM in the MRD show a wide distribution of scales, but they do have differences in dimensions that we interpret to result from different allogenic forcings and the basin's signal-preservation potential. For each time period, the H^*–T^* distributions span high values associated with the smaller coastal channels to smaller values tied to CBs with scales similar to the modern-day Mississippi River. The range and period of RSL cycles in the LM were less than many of the resulting CB thicknesses and the times to generate basin-wide deposits of thicknesses equivalent to the CBs, as $\sim$ 50% of these CBs fall in the signal-shredding regime. However, this result alone does not fully support the shredding of RSL signals in the LM because: 1) half of the CBs in the LM do fall within the signal preservation regime and 2) CBs that fall within the shredding regime could have scales influenced by allogenic signals like RSL change, but

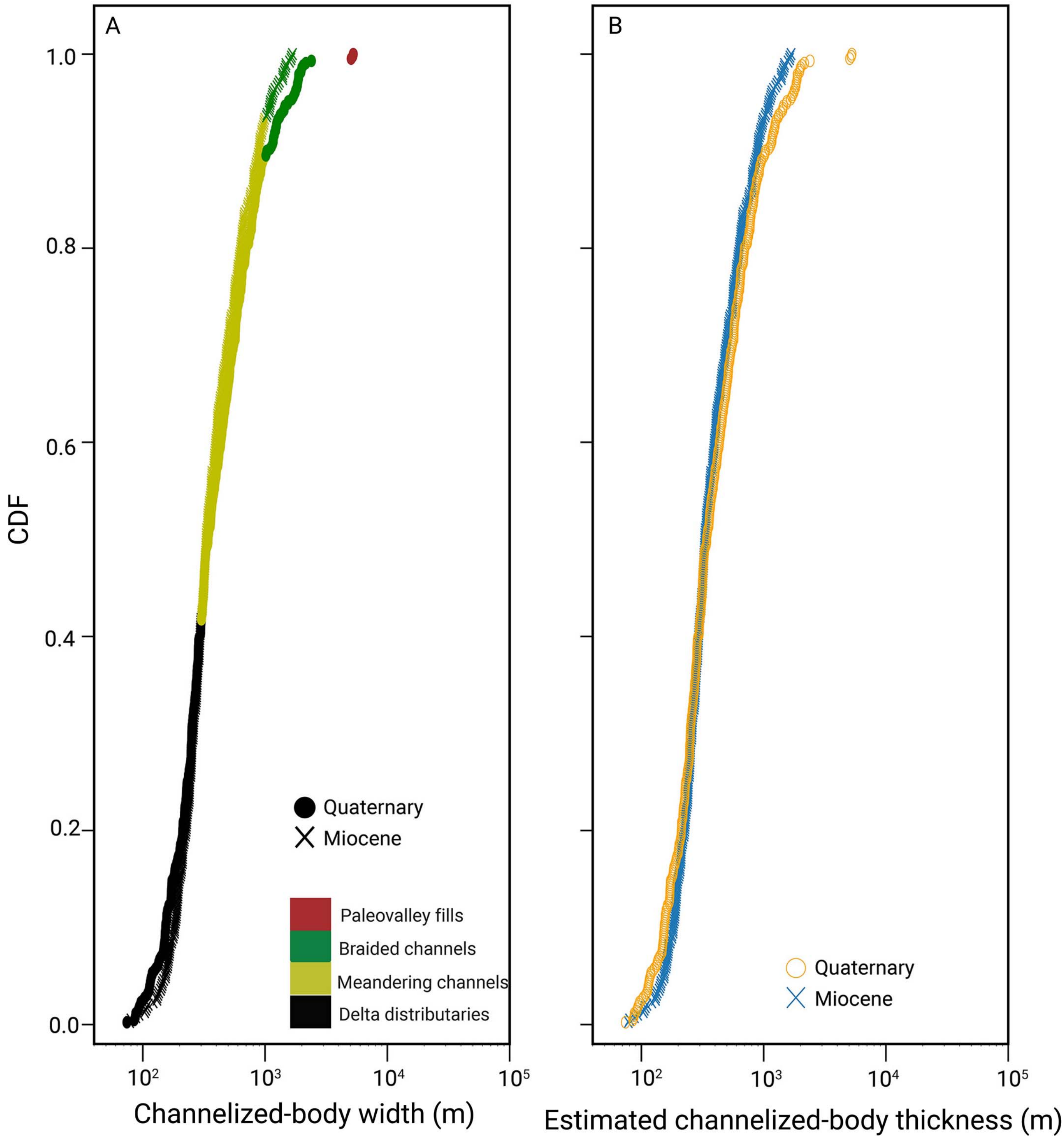

Fig. 6.—A comparison of CB widths and thicknesses for the early Quaternary (shown by circles) and the late Miocene (shown by crosses). **A)** The cumulative distribution function, CDF, of the CB widths. **B)** The CDF of the CB thickness. In both cases, the distributions are similar for the two time periods except for the largest CB features. The early Quaternary has a pronounced heavy tail signifying the presence of paleovalleys, meaning the EQ stratigraphy preserved the RSL signal. We have used a median value for calculating the different types of channelized bodies in this figure, but we acknowledge that these boundaries are gradational in nature.

these signals are obscured by the scale of the autogenic signals and are not statistically detectable.

In contrast, 95% of the EQ CB's fall within the signal-preservation regime of the H^*–T^* plot. This suggests a much higher likelihood that strata of the EQ contain definitive signals of RSL change. Further, of the 5% of EQ CBs that do fall within the shredding regime most have scales more than those found on the modern (autogenic) configuration of the Mississippi River (Nittrouer 2013) and some have width:thickness ratios

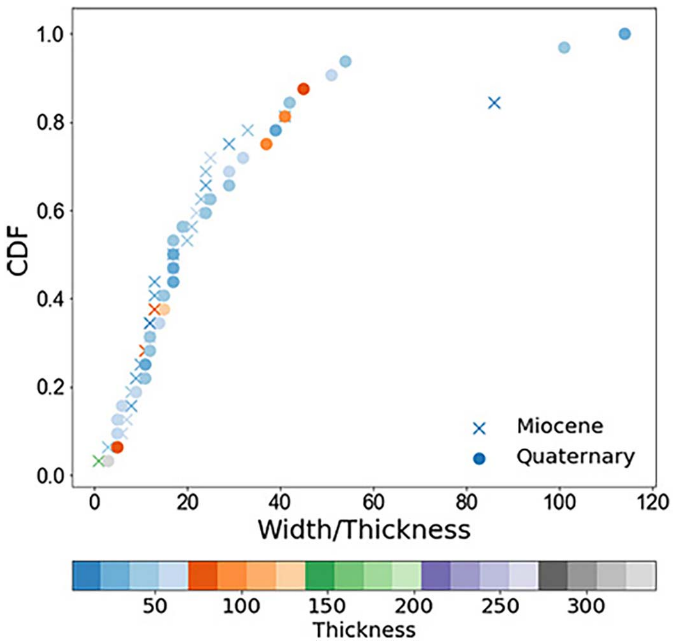

FIG. 7.—The cumulative distribution function of the width-to-thickness ratio of the EQ (shown by circles) and LM (shown by crosses) CBs. CBs are colored according to their thickness.

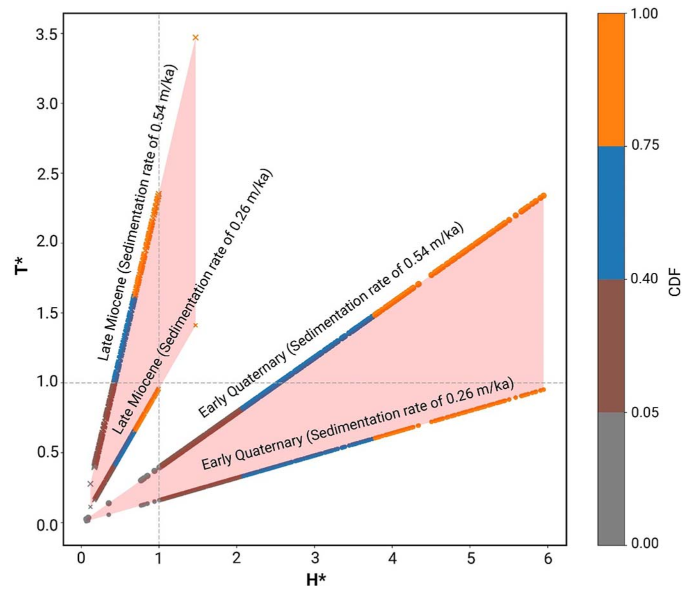

FIG. 8.—H^* and T^* cross plot for CBs of the EQ (shown by circles) and LM (shown by crosses) calculated with two sedimentation rates. The area where H^* and T^* are less than 1 is the shredding regime, and the rest of the space is the preservation regime. Symbols are colored by their distribution CDF values, shown in the color bar. The shaded area in red shows the uncertainty band where the calculated H^* and T^* values can lie with varying input values.

that suggest that they formed during the filling of paleo-valleys carved in response to changing RSL. These observations support signal preservation of changing RSL in EQ strata. This is in line with our predictions based on signal-shredding theory.

We note, though, that all of the mapped CBs in the LM, also have scales that are equal to or less than the scales of the modern-day autogenic Mississippi channel. We do acknowledge that if the Mississippi River were smaller due to the lower sediment and/or water flux due to changes in the hinterland, then the autogenic scales of the past channel would have been smaller than the present-day Mississippi River. Acknowledging uncertainty outlined above, these observations support shredding of signals of RSL change in the LM strata. This is not to disregard the fact that RSL signals might reside in smaller systems akin to the majority of the LM CBs. However, the enhanced scales of width and depth of these smaller systems, as a result of being perturbed by RSL change, might be difficult to identify due to their position in the autogenic distribution of CB dimensions, "obscuring" these environmental signals, instead of shredding them (Griffin et al. 2023). As we see the definitive evidence of RSL signal preservation only in the larger trunk system, our analysis points to the trunk system setting the fidelity of the larger basin.

The LM CBs are not as wide as the present-day Mississippi channel belt when characterized over its final 800 km. However, the widest EQ CBs are also narrower than the present-day Mississippi channel belt over this reach. A second comparison focuses on just the lower 300 km of the modern Mississippi River channel belt. This region is within the backwater reach, where channel belts have scales similar to individual channel features, due to the limited lateral migration rates of channels from loss of bedload at the normal-backwater flow transition (Fernandes et al. 2016; Ganti et al. 2016). We suggest that many of the mapped CBs are individual channel fills, rather than channel-belt fills, given the width-to-depth ratios of features mappable in both time slices and vertical cross sections. This might indicate that they were deposited in backwater reaches, and thus we should compare their scales to modern channel-belt scales in the backwater reach (i.e., lower 300 river km). The widest EQ CBs are of the same width or slightly wider than the modern channel-belt thickness in the lower ~ 300 km. But these CBs are thicker than either the depth of the present-day Mississippi channel or the thickness of the modern channel belt. Thus, we suggest that there is a high probability of these EQ CBs scales being set by allogenic sea-level perturbations, and thus storing RSL signals.

A few of the EQ paleovalleys are estimated to be almost 1 km thick, calculated based on the width:thickness ratio proposed by Gibling (2006). However, what we calculate here are the maximum thicknesses of the CBs and in reality, they must be thinner. This can also provide an uncertainty to the calculation of H* and T*, and by shrinking the CBs, they should plot lower in the H*–T* space. They will in turn fall more towards the shredding regime, making it difficult for stratigraphers to differentiate between the allogenic vs. autogenic forcings in the genesis of these CBs.

The paleovalleys reported in this study are not as wide as is commonly expected for systems comparable to the Mississippi River. The width-to-thickness ratio as well as the width of the CBs identified as paleovalleys are in the lower end of the range of dimensions suggested by Gibling (2006), which are only slightly wider than the modern-day channel-belt dimensions. These paleovalleys are thicker than the average Gulf of Mexico paleovalleys from the last glaciation (Anderson et al. 2016). The width of a paleovalley depends on the number of the channel-belt sandbodies contained in it and their individual widths (Blum et al. 2013). The widest paleovalleys seen here are composed of only a few individual sand bodies whose thicknesses are in the order of 10^1 m, thus restricting the width of the paleovalleys itself (Fig. 4). There can be several reasons behind this, including the sediment flux, the amount of relative sea-level change, its duration, the shelf morphology, and the differences in the basal valley-fill surface (Törnqvist et al. 2006; Blum et al. 2013). However, the aim of this work is to test the signal-shredding theory in an area with field data, and the absence of larger paleovalleys can be restricted by the size of the seismic volume, which would prevent us from mapping larger CBs. For future work, the geographic scale of exploration related to the signal-shredding theory can be a probable avenue to explore.

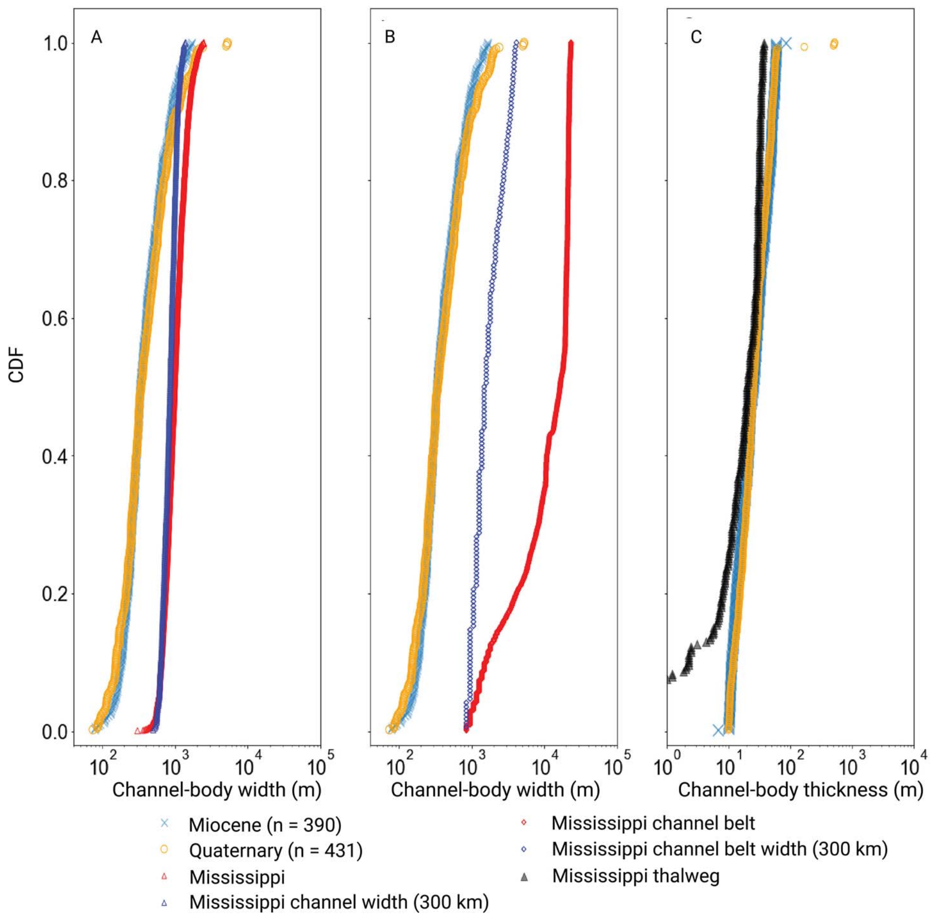

FIG. 9.—Comparing CB widths and thicknesses between the EQ (shown by circles), LM (shown by crosses), and the present-day Mississippi River channel (shown by triangles), and channel belt (shown by diamonds). Cumulative distribution function reported for **A)** the width of LM, EQ, the lower 800 km of the present-day Mississippi River channel, and the lower 200 km (backwater reach) of present-day Mississippi River, **B)** The same as Part A, but instead of the present-day river channel, a comparison with the present-day river channel belt is made. **C)** Estimated EQ, LM CB thickness, and present-day Mississippi River depth. In all comparisons a difference is noted in the positive tail of the distributions, with more weight found in the EQ heavy tail.

The interpreted paleovalleys from the EQ stratigraphy plot in the signal-shredding domain, which probably carry the signals of RSL change (Fig. 8). These geobodies were likely constructed by channels of significant size that were further incised during allogenic RSL change. Channels on the upper end of the autogenic spectrum that responded to large RSL change create the most easily identifiable signal of paleo-RSL change. This contrasts with other smaller-scale channels that were already well within the autogenic band, that when tugged by RSL change deepened and widened, but not out of the autogenic bands. These thick and narrow CBs are most abundant ($H^* < 1$ and $T^* > 1$) for the EQ, which can be a result of autogenic forcing of RSL change, deepening them quickly without enough time for them to widen. The predicted changes in deposition from proximal to distal parts of the system cannot be conclusively tested in this work, due to the limited geographical region explored, and the limited well-log data from the EQ time period, which could aid identification of grain-size signals in the strata. These CBs are conduits of sediment transport to the continental shelf and in time, to the deep marine realm. The competition between the allogenic and autogenic processes during changing RSL cycles on them must have consequences for sediment transport as well. Future work can be focused on this issue as well as other sub-seismic scale-observations.

CONCLUSIONS

This work demonstrates how to apply signal-shredding theory to field-scale settings. Even though numerical and physical experiments have explored signal shredding of RSL change, changing sediment (Toby et al. 2019), or fluid flux (von der Heydt et al. 2003; Jerolmack and Paola 2010; Li et al. 2016; Yu et al. 2017), this is the first test of this idea at field-scale. Using the often underutilized publicly available 3-D seismic volumes from the modern Gulf of Mexico continental shelf, we have compared the identification and preservation of RSL-change signals from two distinct time intervals, early Quaternary and late Miocene. Comparing the CB dimensions from the two time periods and present-day estimates of the Mississippi River, we show that the largest EQ CBs are thicker and wider than both the LM CBs and the present-day Mississippi River CB. Therefore, these large EQ CBs are interpreted as products of the allogenic tug of the RSL, which is lacking in the LM CBs. While we cannot definitively state that signals of RSL change are present or not in either of the two time periods explored, broadly speaking the results support the stratigraphic signal-shredding framework for RSL cycles. This supports the premise that, in some sedimentary basins, some RSL cycles are of insufficient duration or magnitude to produce stratigraphic products outside the range of the products of autogenic channel dynamics. It highlights the need for multiple hypotheses and scenario development that should be considered when interpreting stratal architecture, scales, and geometries for interpretation of global RSL changes.

ACKNOWLEDGMENTS

This study was supported by the National Science Foundation (grant EAR-1424312). We also acknowledge Dr. Zoltan Sylvester for the Python script for calculation of CB dimensions, and Dr. David Mohrig and Dr. Torbjörn Törnqvist for discussions and valuable suggestions. We thank the associate editor Dr. Vamsi Ganti and the two external reviewers, Dr. Ben Cardenas and Dr. Elizabeth Hajek for their comments which have strengthened this manuscript.

SUPPLEMENTAL MATERIALS

Supplemental Materials are available from the SEPM Data Archive: https://www.sepm.org/supplemental-materials.

REFERENCES

Alley, R.B., Clark, P.U., Huybrechts, P., and Joughin, I., 2005, Ice-sheet and sea-level changes: Science, v. 310, p. 456–460.

Anderson, J.B., Wallace, D.J., Simms, A.R., Rodriguez, A.B., Weight, R.W., and Taha, Z. P., 2016, Recycling sediments between source and sink during a eustatic cycle: systems of late Quaternary northwestern Gulf of Mexico Basin: Earth-Science Reviews, v. 153, p. 111–138.

Bentley, S., Blum, M., Maloney, J., Pond, L., and Paulsell, R., 2016, The Mississippi River source-to-sink system: perspectives on tectonic, climatic, and anthropogenic influences, Miocene to Anthropocene: Earth-Science Reviews, v. 153, p. 139–174.

Best, J.L., and Ashworth, P.J., 1997, Scour in large braided rivers and the recognition of sequence stratigraphic boundaries: Nature, v. 387, p. 275–277.

Blum, M.D., and Hattier-Womack, J., 2009, Climate change, sea-level change, and fluvial sediment supply to deepwater depositional systems, *in* Kneller, B., Martinsen, O.J., and McCaffrey, W., eds., External Controls on Deep-Water Depositional Systems: SEPM, Special Publication 92, p. 15–39.

Blum, M., and Pecha, M., 2014, Mid-Cretaceous to Paleocene North American drainage reorganization from detrital zircons: Geology, v. 42, p. 607–610.

Blum, M.D., and Törnqvist, T.E., 2000, Fluvial responses to climate and sea-level change: a review and look forward: Sedimentology, v. 47, p. 2–48.

Blum, M., Martin, J., Milliken, K., and Garvin, M., 2013, Paleovalley systems: insights from Quaternary analogs and experiments: Earth-Science Reviews, v. 116, p. 128–169.

Blum, M.D., Milliken, K.T., Pecha, M.A., Snedden, J.W., Frederick, B.C., and Galloway, W.E., 2017, Detrital-zircon records of Cenomanian, Paleocene, and Oligocene Gulf of Mexico drainage integration and sediment routing: implications for scales of basin-floor fans: Geosphere, v. 13, p. 2169–2205.

Buzas-Stephens, P., Livsey, D.N., Simms, A.R., and Buzas, M.A., 2014, Estuarine foraminifera record Holocene stratigraphic changes and Holocene climate changes in ENSO and the North American monsoon: Baffin Bay, Texas: Palaeogeography, Palaeoclimatology, Palaeoecology, v. 404, p. 44–56.

Cardenas, B.T., Lamb, M.P., Jobe, Z.R., Mohrig, D., and Swartz, J.M., 2023, Morphodynamic preservation of fluvial channel belts: The Sedimentary Record, v. 21, doi:10.2110/001c.66285.

Catuneanu, O., Abreu, V., Bhattacharya, J.P., Blum, M.D., Dalrymple, R.W., Eriksson, P.G., Fielding, C.R., Fisher, W.L., Galloway, W.E., Gibling, M.R., Giles, K.A., Holbrook, J.M., Jordan, R., Kendall, C.G.St.C., Macurda, B., Martinsen, O.J., Miall, A.D., Neal, J.E., Nummedal, D., Pomar, L., Posamentier, H.W., Pratt, B.R., Sarg, J.F., Shanley, K.W., Steel, R.J., Strasser, A., Tucker, M.E., and Winker, C., 2009, Towards the standardization of sequence stratigraphy: Earth-Science Reviews, v. 92, p. 1–33.

Clark, P.U., McCabe, A.M., Mix, A.C., and Weaver, A.J., 2004, Rapid rise of sea level 19,000 years ago and its global implications: Science, v. 304, p. 1141–1144.

Combellas-Bigott, R.I., and Galloway, W.E., 2006, Depositional and structural evolution of the middle Miocene depositional episode, east-central Gulf of Mexico: American Association of Petroleum Geologists, Bulletin, v. 90, p. 335–362.

Diegel, F.A., Karlo, J., Schuster, D., Shoup, R., and Tauvers, P., 1995, Cenozoic structural evolution and tectono-stratigraphic framework of the northern Gulf Coast continental margin, *in* Jackson, M.P.A., Roberts, D.G., and Snelson, S., eds., Salt Tectonics: A Global Perspective: American Association of Petroleum Geologists, Memoir 65, p. 109–151.

Fairbanks, R.G., 1989, A 17,000-year glacio-eustatic sea-level record: influence of glacial melting rates on the Younger Dryas event and deep-ocean circulation: Nature, v. 342, p. 637–642.

Fernandes, A.M., Törnqvist, T.E., Straub, K.M., and Mohrig, D., 2016, Connecting the backwater hydraulics of coastal rivers to fluvio-deltaic sedimentology and stratigraphy: Geology, v. 44, p. 979–982.

Fisk, N.H., and, McFarlan, E., 1955, Late Quaternary deltaic deposits of the Mississippi River: Geological Society of America, Special Paper 62, p. 279–302.

Galloway, W.E., 2008, Depositional evolution of the Gulf of Mexico sedimentary basin: Sedimentary Basins of the World, v. 5, p. 505–549.

Galloway, W.E., Ganey-Curry, P.E., Li, X., and Buffler, R.T., 2000, Cenozoic depositional history of the Gulf of Mexico basin: American Association of Petroleum Geologists, Bulletin, v. 84, p. 1743–1774.

Galloway, W.E., Whiteaker, T.L., and Ganey-Curry, P., 2011, History of Cenozoic North American drainage basin evolution, sediment yield, and accumulation in the Gulf of Mexico basin: Geosphere, v. 7, p. 938–973.

Ganti, V., Chu, Z., Lamb, M.P., Nittrouer, J.A., and Parker, G., 2014, Testing morphodynamic controls on the location and frequency of river avulsions on fans versus deltas: Huanghe (Yellow River), China: Geophysical Research Letters, v. 41, p. 7882–7890.

Ganti, V., Chadwick, A.J., Hassenruck-Gudipati, H.J., Fuller, B.M., and Lamb, M.P., 2016, Experimental river delta size set by multiple floods and backwater hydrodynamics: Science Advances, v. 2, no. e1501768.

Ganti, V., Lamb, M.P., and Chadwick, A.J., 2019, Autogenic erosional surfaces in fluvio-deltaic stratigraphy from floods, avulsions, and backwater hydrodynamics: Journal of Sedimentary Research, v. 89, p. 815–832.

Gibling, M.R., 2006, Width and thickness of fluvial channel bodies and valley fills in the geological record: a literature compilation and classification: Journal of Sedimentary Research, v. 76, p. 731–770.

Griffin, C., Duller, R.A., and Straub, K.M., 2023, The degradation and detection of environmental signals in sediment transport systems: Science Advances, v. 9, no. eadi8046.

Haq, B.U., 1991, Sequence stratigraphy, sea-level change, and significance for the deep sea, *in* Macdonald, D.I.M., ed., Sedimentation, Tectonics and Eustasy: International Association of Sedimentologists, Special Publication 12, p. 1–39.

Haq, B.U., Hardenbol, J., and Vail, P.R., 1987, Chronology of fluctuating sea levels since the Triassic: Science, v. 235, p. 1156–1167.

Imbrie, J., and Imbrie, J.Z., 1980, Modeling the climatic response to orbital variations: Science, v. 207, p. 943–953.

Jerolmack, D.J., and Paola, C., 2010, Shredding of environmental signals by sediment transport: Geophysical Research Letters, v. 37, no. L19401.

Khan, N.S., Horton, B.P., Engelhart, S., Rovere, A., Vacchi, M., Ashe, E.L., Törnqvist, T.E., Dutton, A., Hijma, M.P., and Shennan, I., 2019, Inception of a global atlas of sea levels since the Last Glacial Maximum: Quaternary Science Reviews, v. 220, p. 359–371.

Lamb, M.P., Nittrouer, J.A., Mohrig, D., and Shaw, J., 2012, Backwater and river plume controls on scour upstream of river mouths: implications for fluvio-deltaic morphodynamics: Journal of Geophysical Research, Earth Surface, v. 117, p. F01002.

Leopold, L.B., and Wolman, M.G., 1960, River meanders: Geological Society of America, Bulletin, v. 71, p. 769–793.

Li, Q., Yu, L., and Straub, K.M., 2016, Storage thresholds for relative sea-level signals in the stratigraphic record: Geology, v. 44, p. 179–182.

Lisiecki, L.E., and Raymo, M.E., 2005, A Pliocene–Pleistocene stack of 57 globally distributed benthic delta O-18 records: Paleoceanography, v. 20, PA1003.

Miller, K.G., Kominz, M.A., Browning, J.V., Wright, J.D., Mountain, G.S., Katz, M.E., Sugarman, P.J., Cramer, B.S., Christie-Blick, N., and Pekar, S.F., 2005, The Phanerozoic record of global sea-level change: Science, v. 310, p. 1293–1298.

Mohrig, D., Heller, P.L., Paola, C., and Lyons, W.J., 2000, Interpreting avulsion process from ancient alluvial sequences: Guadalope–Matarranya (northern Spain) and Wasatch Formation (western Colorado): Geological Society of America, Bulletin, v. 112, p. 1787–1803.

Nittrouer, J.A., 2013, Backwater hydrodynamics and sediment transport in the lowermost Mississippi River Delta: implications for the development of fluvial–deltaic landforms in a large lowland river, *in* Young, F.J., Perillo, G.M.E., Aksoy, H., Bogen, J., Gelfan, A., Mahé, G., Marsh, P., and Savenije, H.H.G., eds., Deltas: Landforms, Ecosystems, and Human Activities: International Association of Hydrological Sciences, Assembly, Proceedings, v. 358, p. 48–61.

Olariu, C., and Bhattacharya, J.P., 2006, Terminal distributary channels and delta front architecture of river-dominated delta systems: Journal of Sedimentary Research, v. 76, p. 212–233.

Olariu, C., and Steel, R.J., 2009, Influence of point-source sediment-supply on modern shelf-slope morphology: implications for interpretation of ancient shelf margins: Basin Research, v. 21, p. 484–501.

Peel, F.J., 2014, How do salt withdrawal minibasins form? Insights from forward modelling, and implications for hydrocarbon migration: Tectonophysics, v. 630, p. 222–235.

Peel, F., Travis, C., and Hossack, J., 1995, Genetic structural provinces and salt tectonics of the Cenozoic offshore US Gulf of Mexico: a preliminary analysis, *in* Jackson, M.P.A., Roberts, D.G., and Snelson, S., eds., Salt Tectonics: a Global Perspective: American Association of Petroleum Geologists, Memoir, v. 65, p. 153–175.

Posamentier, H.W., and Vail, P.R., 1988, Eustatic controls on clastic deposition I, sequence and systems tract models, *in* Wilgus, C.K., Hastings, B.S., Kendall, C.G.St.C., Posamentier, H.W., Ross, C.A., and Van Wagoner, J.C., eds., Sea-Level Changes: An Integrated Approach: SEPM, Special Publication 42, p. 125–154.

Posamentier, H.W., Allen, G.P., and James, D.P., 1992, High resolution sequence stratigraphy: the East Coulee Delta, Alberta: Journal of Sedimentary Research, v. 62, p. 310–317.

Raymo, M.E., Lisiecki, L., and Nisancioglu, K.H., 2006, Plio-Pleistocene ice volume, Antarctic climate, and the global δ^{18}O record: Science, v. 313, p. 492–495.

Romans, B.W., Castelltort, S., Covault, J.A., Fildani, A., and Walsh, J., 2016, Environmental signal propagation in sedimentary systems across timescales: Earth-Science Reviews, v. 153, p. 7–29.

Straub, K.M., Paola, C., Mohrig, D., Wolinsky, M.A., and George, T., 2009, Compensational stacking of channelized sedimentary deposits: Journal of Sedimentary Research, v. 79, p. 673–688.

Straub, K.M., Duller, R.A., Foreman, B.Z., and Hajek, E.A., 2020, Buffered, incomplete, and shredded: the challenges of reading an imperfect stratigraphic record: Journal of Geophysical Research, Earth Surface, v. 125, no. e2019JF005079.

Swartz, J.M., Cardenas, B.T., Mohrig, D., and Passalacqua, P., 2022, Tributary channel networks formed by depositional processes: Nature Geoscience, v. 15, p. 216–221.

Sylvester, Z., Durkin, P.R., Hubbard, S.M., and Mohrig, D., 2021, Autogenic translation and counter point bar deposition in meandering rivers: Geological Society of America, Bulletin, v. 133, p. 2439–2456.

Törnqvist, T.E., Wortman, S.R., Mateo, Z.R.P., Milne, G.A., and Swenson, J.B., 2006, Did the last sea-level lowstand always lead to cross-shelf valley formation and source-to-sink sediment flux?: Journal of Geophysical Research, Earth Surface, v. 111, p. F04002.

Tornqvist, T.E., Wallace, D.J., Storms, J.E.A., Wallinga, J., Van Dam, R.L., Blaauw, M., Derksen, M.S., Klerks, C.J.W., Meijneken, C., and Snijders, E.A., 2008, Mississippi Delta subsidence primarily caused by compaction of Holocene strata: Nature Geoscience, v. 1, p. 173–176.

Trampush, S., Hajek, E., Straub, K., and Chamberlin, E., 2017, Identifying autogenic sedimentation in fluvial-deltaic stratigraphy: evaluating the effect of outcrop-quality data on the compensation statistic: Journal of Geophysical Research, Earth Surface, v. 122, p. 1–23.

Trower, E.J., Ganti, V., Fischer, W.W., and Lamb, M.P., 2018, Erosional surfaces in the Upper Cretaceous Castlegate Sandstone (Utah, USA): sequence boundaries or autogenic scour from backwater hydrodynamics?: Geology, v. 46, p. 707–710.

Voller, V.R., Ganti, V., Paola, C., and Foufoula-Georgiou, E.V., 2012, Does the flow of information in a landscape have direction?: Geophysical Research Letters, v. 39, no. L01403.

Von Der Heydt, A., Grossmann, S., and Lohse, D., 2003, Response maxima in modulated turbulence. II. Numerical simulations: Physical Review E, v. 68, no. 066302.

Wang, Y., Straub, K.M., and Hajek, E.A., 2011, Scale-dependent compensational stacking: an estimate of autogenic time scales in channelized sedimentary deposits: Geology, v. 39, p. 811–814.

Winker, C.D., 1982, Cenozoic shelf margins, northwestern Gulf of Mexico: Gulf Coast Association of Geological Societies, Transactions, v. 32, p. 427–448.

Xu, J., Snedden, J.W., Galloway, W.E., Milliken, K.T., and Blum, M.D., 2017, Channel-belt scaling relationship and application to early Miocene source-to-sink systems in the Gulf of Mexico basin: Geosphere, v. 13, p. 179–200.

Yu, L., Li, Q., and Straub, K.M., 2017, Scaling the response of deltas to relative-sea-level cycles by autogenic space and time scales: a laboratory study: Journal of Sedimentary Research, v. 87, p. 817–837.

Received 20 February 2024; accepted 18 December 2024.